applied sciences

MDPI

Article

A Novel Modular Multi-Unit Cell Permanent Magnet Thrust Bearing with Bionic Design and Load-Carrying Capacity Analysis

Xiangdong Yu [1], Qi Wang [2], Zhongsheng Yan [1], Wenfeng Yu [1], Xingyue Shang [2], Suimeng Zhou [2] and Jimin Zhang [2,*]

[1] Power Plant Division, Shanghai Marine Diesel Engine Research Institute, Shanghai 201108, China; yuxiangd711@163.com (X.Y.)
[2] College of Transportation, Tongji University, Shanghai 201804, China
* Correspondence: zjm2011@tongji.edu.cn; Tel.: +86-136-3656-6657

Abstract: Permanent magnet thrust bearings have garnered significant attention due to their high rotational speeds, low noise levels, and excellent vibration-damping performance. However, existing designs of these bearings often suffer from low load-carrying capacity and are tailored to specific machines, which limits their broader applicability. To address these limitations, this paper proposes a novel modular multi-unit cell structure for permanent magnet thrust bearings. The load-carrying performance of this design is validated through theoretical analysis, simulation, and experimentation. The inspiration for this design comes from bionics and honeycomb structures, emphasizing modularization and the combination of multiple unit cells. The unit cell consists of four permanent magnets, and multiple unit cells can be connected to form a structure that replaces the traditional design of directly embedding a permanent magnet ring into the bearing structure. Moreover, the designed unit cell structure can expand in both axial and radial directions, allowing for the creation of various nested or cross structures tailored to specific usage requirements. With this modular approach, the theoretical model of the bearing structure can be extended from the traditional single-layer cross-nested structure to an arbitrary number of nested cross-nested configurations using the equivalent magnetic circuit method. The bearing's performance is validated through finite element simulations and experimental testing. The results demonstrate that the bearing with a four-layer cross-nested structure achieves a maximum load capacity of 48.45 kN, with a deviation of 7.3% from the theoretical value and 4% from the simulation results. By leveraging the generalization of the unit cell, the maximum axial load capacity across various configurations ranges from 6.78 kN to 288.9 kN, significantly enhancing the bearing's adaptability to diverse operational scenarios.

Keywords: permanent magnet thrust bearing; bionic design; multilayer nested crossover; theoretical model; finite element analysis; experimental verification

check for updates

Academic Editor: Alberto Benato

Received: 17 February 2025
Revised: 10 March 2025
Accepted: 22 March 2025
Published: 3 April 2025

Citation: Yu, X.; Wang, Q.; Yan, Z.; Yu, W.; Shang, X.; Zhou, S.; Zhang, J. A Novel Modular Multi-Unit Cell Permanent Magnet Thrust Bearing with Bionic Design and Load-Carrying Capacity Analysis. *Appl. Sci.* **2025**, *15*, 3926. https://doi.org/10.3390/app15073926

Copyright: © 2025 by the authors. Licensee MDPI, Basel, Switzerland. This article is an open access article distributed under the terms and conditions of the Creative Commons Attribution (CC BY) license (https://creativecommons.org/licenses/by/4.0/).

1. Introduction

Modern advanced ship propulsion systems have put forward more stringent requirements for acoustic stealth [1]. In the process of ship propulsion, the thrust bearing is a crucial component for transmitting propulsive force to the hull, and its vibrations can lead to resonance throughout the entire hull structure. Consequently, there has been a significant increase in the development of vibration-damping thrust bearings, both domestically and internationally. Currently, the primary methods for reducing vibration and noise include rubber vibration damping [2], hydraulic vibration damping [3], and polymer material

vibration damping [4], among others. These techniques have achieved some success, particularly in minimizing vibrations in the middle and high-frequency ranges. However, the effectiveness of vibration damping in the middle and low-frequency bands has not yet met expectations. As a result, there is an urgent need to explore new technologies to enhance the acoustic stealth of thrust bearings, particularly in improving vibration and noise reduction capabilities in the middle and low-frequency ranges.

Permanent magnet thrust bearings offer a natural advantage in vibration and noise reduction. They utilize the magnetic force generated by permanent magnets to achieve contactless levitation of the rotor, enabling the rotor and stator to remain mutually separated without the need for lubrication or friction during operation. This unique feature makes permanent magnet thrust bearings especially suitable for use in contactless transmission systems, such as spacecraft [5], flywheel energy storage systems [6], and high-precision machine tools [7]. Due to their contactless operation, permanent magnet thrust bearings provide key advantages, including frictionless motion, low noise, and high-speed capabilities.

Given the excellent performance of permanent magnet bearings, many researchers have focused on various aspects, such as bearing structure design, bearing capacity, stiffness, optimization, and experimental methods. In flywheel energy storage systems, permanent magnet bearings have shown promising application prospects and have attracted considerable attention. One study [8] proposed a numerical method for the structural design of a new type of permanent magnet bearing for flywheel energy storage systems, enabling rapid determination of the bearing's force, stiffness, and damping characteristics, which was experimentally validated. Another study [6] introduced a system utilizing both superconducting magnetic bearings and permanent magnet bearings, where superconducting magnetic bearings suppress the vibration of the flywheel rotor while permanent magnet bearings passively control the rotor's position, demonstrating excellent control effectiveness.

To improve the bearing capacity of permanent magnet bearings, another approach [9] combined permanent magnet bearings with fluid bearing technology. This approach explores the possibility of achieving both low starting torque in permanent magnet bearings and high bearing capacity in fluid bearings under a single-bearing arrangement. Experimental results have shown an improvement in bearing capacity. In centrifuge rotating bearings, which are subjected to extreme working conditions such as high rotational speeds, traditional contact bearings are prone to metal fatigue, cracks, and other failures that compromise their operational lifespan. To address this, one study [10] proposed a centrifuge-specific permanent magnetic bearing, leveraging the non-contact nature of permanent magnetic bearings to achieve high rotational speeds and extend bearing life.

The bearing capacity and stiffness of permanent magnet bearings are crucial mechanical characteristics. To investigate how structural parameters—such as thickness, width, number of layers, cross-sectional area, and air gap—affect the mechanical properties of radially magnetized permanent magnet bearings, researchers [11] conducted in-depth studies, providing valuable insights into structural design. To address the challenges associated with the complex structure, intricate design, and difficult processing and assembly of permanent magnet bearings, another paper [12] proposed a modular permanent magnet bearing. This work introduced the bearing's operating principle and examined its performance through computer simulations.

The widespread use of composite materials also opens up new possibilities for the structural design of permanent magnet bearings. One study [13] proposed a new type of composite material used to construct a permanent magnet bearing applied in a bevel gear-coupled rotor system. This study involved the optimization of structural parameters, analysis of the magnetic field, and assessment of dynamic stiffness in the permanent magnet bearings, demonstrating the advantages of composite material applications. Additionally,

optimized design remains a key strategy for improving bearing load-carrying performance. Another study [14] introduced a simplified numerical method to predict the performance of various permanent magnet bearings and subsequently optimized parameters such as the number of permanent magnet rings and the air gap.

Permanent magnet motors represent another key application of permanent magnet drive systems. The design of permanent magnet bearings is influenced by several factors, including the arrangement of permanent magnets, the materials used, the method of embedding, the shape of the magnets, and the application of finite element analysis techniques. To investigate the impact of different magnet arrangements on the performance of permanent magnet motors, researchers [15] constructed three different types of permanent magnet motors, analyzed their performance using finite element analysis, and calibrated the output power range for each configuration. The choice of material also significantly impacts the performance of permanent magnet motors. Research referenced in [16] investigated the effect of using different permanent magnet materials, examining how variations in the number of materials influence motor characteristics through finite element simulations, thus revealing the complex relationship between the material properties and motor performance. Additionally, nanostructured permanent magnet materials are considered a promising option for the next generation of high-strength permanent magnets. However, the mass production of nano-sized permanent magnets remains challenging, as traditional sintering processes are unable to produce nano-sized permanent magnets directly. The authors of [17] reviewed the research progress in aspects such as grain size control, interface modification, and the generation of anisotropy of nano permanent magnets, providing certain guidance for the manufacturing and application of nano permanent magnets. Due to the high cost of permanent magnet materials, the expense of using a large number of permanent magnets in propulsion systems is often economically unfeasible. To address this, [18] introduced an innovative approach to reduce the number of permanent magnets required to create a permanent magnet drive train. This method, which minimizes or eliminates the use of rare-earth permanent magnet materials, led to significant cost savings while still meeting performance requirements. When analyzing permanent magnet rotational systems using the finite element method (FEM), the enormous computational volume often consumes considerable resources. To overcome this, [19] proposes a new optimization algorithm that constructs a high-precision agent model while reducing the need for extensive FEM analysis. The optimization results and the accuracy of the FEM analysis are subsequently verified through experiments, demonstrating the efficacy of this approach in improving computational efficiency.

Through the above literature review, it is clear that in the field of permanent magnet drive systems, particularly permanent magnet thrust bearings, numerous scholars have made significant progress in areas such as overall structure design, magnet arrangement, theoretical analysis, finite element simulation, and experimental validation. Moreover, related engineering applications are also being actively explored. However, it is important to note that the traditional structure of permanent magnet thrust bearings often exhibits a lack of diversity. Many existing bearings fail to demonstrate generalizability and scalability, limiting their adaptability across different systems and applications. This presents a clear and pressing need for innovative approaches to develop more versatile, modular, and scalable permanent magnet thrust bearings.

In summary, the limitations of the existing permanent magnet thrust bearing design are as follows:

(1) Permanent magnet thrust bearings typically adopt the method of embedding permanent magnet rings directly into the bearing structure [6]. This makes the assembly process more complex. Furthermore, if a single magnet is damaged, due to its direct

embedding in the bearing mechanism, the damaged magnet could lead to secondary damage to the bearing structure and other magnets.

(2) Existing permanent magnet thrust bearings are often designed for specific machines [20]. Their size, structure, and bearing capacity are tailored to meet the current design requirements, resulting in a lack of generalization and serialization capabilities. Additionally, their load-bearing capacity is often low, making them unsuitable for high-demand applications such as ship spindle propulsion.

(3) The theoretical models for permanent magnet thrust bearings are usually limited to single-layer cross-nested structures [21]. There is a notable deficiency of well-defined theoretical models for multi-layer cross-nested structures. Moreover, the data on bearing capacity are commonly derived from theoretical calculations and simulations, often lacking rigorous experimental validation.

To address these limitations, this paper proposes a novel modular multi-unit cell permanent magnet thrust bearing. The research framework is depicted in Figure 1, with the following contributions:

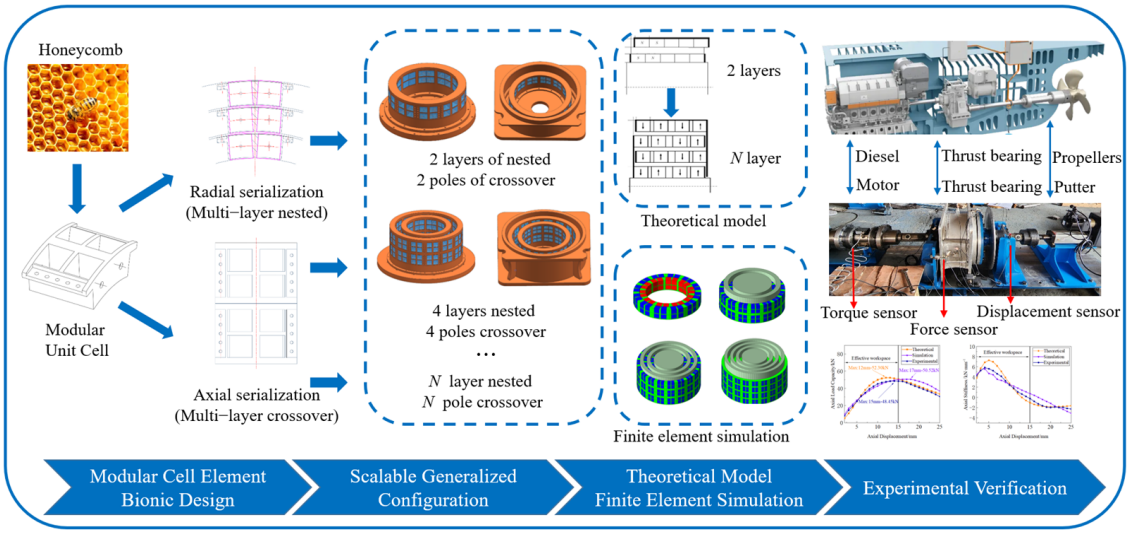


Figure 1. The main architecture of this paper.

(1) Drawing inspiration from bionics and the honeycomb structure, a modular approach is adopted that incorporates a unit cell consisting of four permanent magnets. The design replaces the traditional permanent magnet ring, which is directly embedded in the bearing structure, with multiple connected unit cells. This separation allows the magnets to be isolated from one another, improving both durability and performance.

(2) By generalizing the unit cell structure and varying the number and arrangement of multiple unit cells, a flexible design with multiple nested and cross structures can be realized. This modular design enables the creation of a multi-unit cell permanent magnet thrust bearing adaptable to different configurations and requirements.

(3) The theoretical model for multi-layer cross-nested permanent magnet thrust bearings is derived and calculated based on the principles of virtual displacement and virtual work. This extension broadens the applicability of traditional models, which were previously limited to single-layer cross-nested structures, allowing for multi-layer cross-nested configurations. Additionally, an experimental platform for the permanent magnet thrust bearing is designed with a focus on ship spindle propulsion, and experimental validation is carried out to confirm the theoretical findings.

The main contents of this paper are organized as follows: Section 1 is the introduction; Section 2 outlines the structural design of a modular multi-unit cell permanent magnet

thrust bearing, describing the general structure of the proposed permanent magnet thrust bearing, the magnet embedding and assembling methods, and the detailed structure of the magnet mounting baskets; Section 3 provides the magnetic circuit analysis and theoretical calculations, describing the magnetic circuit of the proposed permanent magnet thrust bearing design, and the theoretical model of the multi-layer cross-nested structure is given through the principle of virtual displacement and the principle of linear superposition; Section 4 includes the simulation analysis, in which, through the commercial finite element simulation software, a variety of cross-nested structures of the permanent magnet thrust bearing model are established, and the simulation work carried out according to the actual use of the working conditions; Section 5 describes the experimental validation, in which an experimental platform for the permanent magnet thrust bearing is constructed, a prototype of the four-level nested quadrupole cross bearing is developed, and experimental tests are carried out; and Section 6 is the conclusion.

2. Structural Design of Modular Multi-Unit Cell Permanent Magnet Thrust Bearing

2.1. General Design

Conventional permanent magnet thrust bearings typically use permanent magnet rings or permanent magnets directly embedded into the main bearing structure. While this design approach is simple and involves fewer parts, it has certain limitations. Due to the large size of the permanent magnet ring, assembly becomes challenging. Furthermore, in the event of magnet damage, the lack of isolation between the permanent magnets can lead to secondary damage to the bearing structure, resulting in the need to scrap the entire bearing, as illustrated in Figure 2. In normal conditions, magnet replacement is also extremely difficult, requiring complete disassembly of the entire bearing. This significantly limits the practical engineering applications of permanent magnet thrust bearings. In addition to the poor generalization and maintainability of such bearings, another major issue restricting their broader use is their low load-carrying capacity. Conventional permanent magnet thrust bearings often adopt a two-layer nested structure, with the rotor's permanent magnets in the inner layer and the stator's permanent magnets in the outer layer, as shown in Figure 3. While this structure has the advantage of a simpler design, its two-layer nested configuration, featuring two layers of permanent magnets alongside a single working surface, limits the efficient use of the magnets' magnetic force. As a result, the load-carrying capacity is relatively modest. Therefore, it is primarily suitable for low load-bearing applications, such as in high-precision instruments, where a high load capacity is not essential.

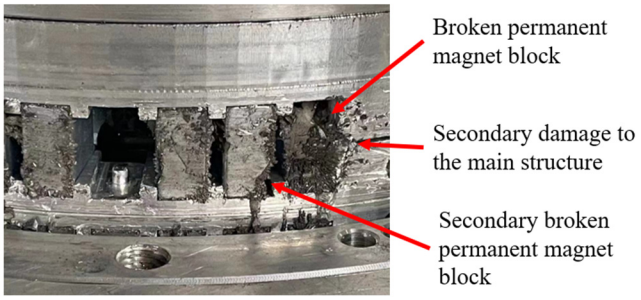


Figure 2. Broken permanent magnet thrust bearing.

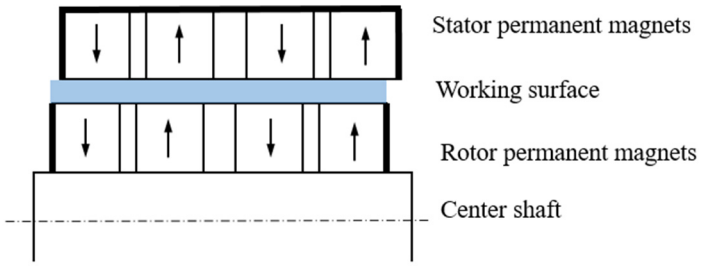


Figure 3. Conventional single-layer permanent magnet thrust bearing. The arrows in the diagram represent the direction of the magnetic lines of force.

To improve the adaptability of permanent magnet thrust bearings in various scenarios and enhance the versatility of the bearing structure, a new approach is proposed. This design is based on the concept of bionics and references the honeycomb structure. By adopting the modular concept and utilizing a multi-unit cell combination approach, where each unit cell is composed of four permanent magnets, and referring to the basic structure of the permanent magnet thrust bearing, the original method of directly embedding permanent magnets or permanent magnet rings into the structure is changed to one involving the connection of multiple unit cells. The number and arrangement of these unit cells can be adjusted to achieve various nested and cross configurations. This flexibility allows for the design of modular, multi-unit cell permanent magnet thrust bearings. One such example is the four-layer nested four-pole crossover bearing design, as shown in Figure 4. In operation, the magnetic force of the permanent magnets allows the rotor and stator to levitate without direct contact. When axial forces are applied, the bearing rotor experiences a slight axial displacement. The attraction and repulsion forces of the permanent magnets maintain stable levitation, ensuring smooth operation without friction. This design improves the load-carrying capacity and enhances the adaptability of the thrust bearing across a wide range of applications.

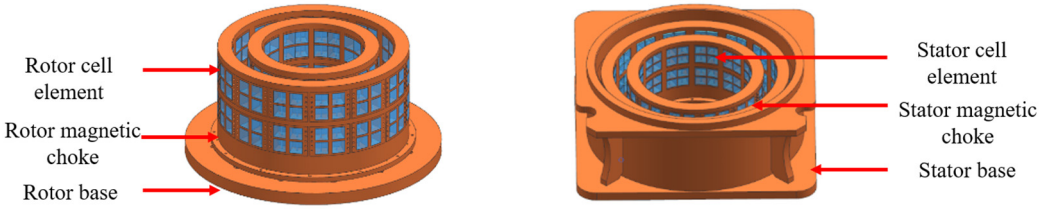


Figure 4. Modular multi-unit cell permanent magnet thrust bearing with four-layer nested and four-pole crossover.

The modular multi-unit cell permanent magnet thrust bearing consists of a rotor and stator housing, rotor and stator chokes, and multiple unit cells. The rotor and stator housings feature a disk-type design, while the rotor and stator chokes are bolted to these housings. These circular chokes contain multiple square openings to accommodate the unit cells, which are bolted to the chokes. Shock-absorbing rubber cushions are employed to reduce vibrations. When the size and load-carrying capacity of the bearing have different requirements, the size of the bearing housings and chokes can be changed, which in turn alters the number and arrangement of the unit cells. This enables the realization of a universal configuration ranging from the two-layer nested two-pole crossover to an eight-layer nested eight-pole crossover, ultimately allowing the bearing to achieve different load-carrying characteristics based on specific requirements.

The modular multi-unit cell permanent magnet thrust bearings offer easy assembly and maintenance, thanks to the generalization and serialization enabled by the unit cell combination. During assembly, the modular design of the cells reduces the workload and

increases assembly efficiency. When in use, the isolated magnets—thanks to the unit cell structure—prevent damage to a single magnet from affecting other magnets or the core bearing mechanism, thus reducing the frequency and extent of maintenance. Moreover, when replacing or maintaining the permanent magnets, it is unnecessary to disassemble the entire system. Instead, only the damaged cell needs to be replaced, significantly lowering maintenance costs.

2.2. Generalized Unit Cell Configurations

The unit cell of the permanent magnet thrust bearing adopts a generalized configuration, with the basic structure shown in Figure 5. The unit cell primarily consists of a block mounting basket, permanent magnets, vibration-damping rubber pads, and other components. The permanent magnets used are NdFeB magnets of grade N48, with each magnet measuring 30 × 28 × 25 mm and having a remanent magnetization strength of 1.4 T. Compared to other magnetic materials, NdFeB has a higher magnetic energy product and produces more magnetic energy in the same volume. The magnets are housed within the block mounting basket to isolate them from one another. This configuration ensures that each magnet remains separate, preventing interference and damage to adjacent magnets. The unit cells are then bolted together as an integrated unit and mounted onto the rotor and stator chokes of the bearing. Vibration-damping rubber pads are incorporated to absorb shocks and mitigate vibrations during operation, enhancing the overall performance and longevity of the bearing system.

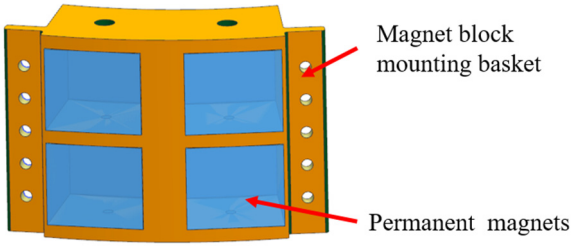


Figure 5. Modularized unit cell structure.

2.3. Expandable Bearing Structure

A typical modular multi-unit cell permanent magnet thrust bearing features a four-layer nested four-pole crossover stacked structure. By varying the number and arrangement of the unit cells, permanent magnet bearings can be configured with two, four, six, or eight levels of nesting and two, four, six, or eight levels of crossover. When a greater axial load-carrying capacity is required, under the premise of meeting the size requirements, the number of nesting layers and cross poles of the bearing can be increased. The structure of the unit cells is universal when the difference in inner and outer diameters is the same. This modular multi-cell design improves the design and manufacturing efficiency of the bearing structure, while also meeting the requirements of different load-carrying capacities. An example of the bearing structure with two layers of nesting and a bipolar cross structure for the same difference in inner and outer diameters is shown in Figure 6.

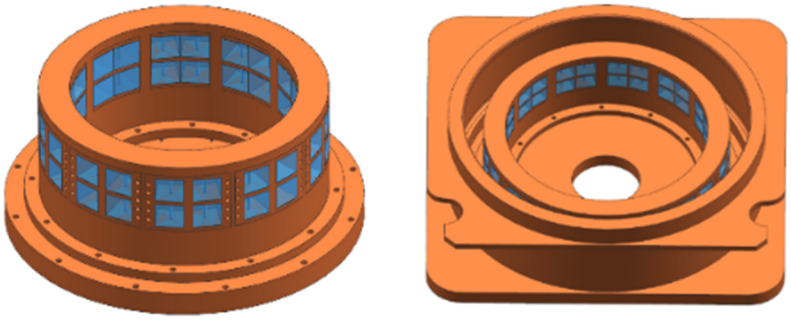


Figure 6. Modular multi-unit cell permanent magnet thrust bearing with two-layer nested two-pole crossover.

3. Magnetic Circuit Design and Theoretical Modeling

3.1. Magnetic Circuit Design

The magnetic circuit is a critical component of permanent magnet thrust bearings, as it directly influences the bearing's load-carrying performance. Traditional permanent magnet thrust bearings typically adopt a single-layer nested design with two layers of magnets and one layer of the working surface. This configuration results in lower magnet utilization and, consequently, a reduced bearing capacity.

In contrast, the modular multi-unit cell permanent magnet thrust bearing proposed in this paper allows for the realization of cross-nested structures with different layers by adding multi-layer rotor and stator magnetic chokes in the radial direction. Axially, the bearing can accommodate multiple layers of unit cells by extending the lengths of the rotor and stator magnetic chokes. This design enables the creation of structures with various pole crossovers. By changing the number and arrangement of the unit cells, the modular multi-unit cell permanent magnet thrust bearing can achieve configurations such as two, four, six, or eight layers of nested structures, as well as two-pole, four-pole, six-pole, and eight-pole crossovers. This flexibility improves the bearing's adaptability, all while maintaining the generalization of the unit cells. The basic structure of the magnetic circuit for the modular multi-unit cell permanent magnet thrust bearing with a four-layer nested four-pole crossover is shown in Figure 7. In this configuration, the diameter of the central axis is denoted by d, the radial thickness of the permanent magnet is d_1, the axial length is l, the width of the air gap is g, and the maximum diameter is D. During operation, the inner ring of the bearing experiences an axial offset e under axial force. The inner ring is subjected to the attractive and repulsive forces of the permanent magnets, which stabilizes the axial position of the thrust bearing. Additionally, the magnetic circuit design employs radial magnetization, with magnetic lines of force distributed radially within the air gap of the magnetic ring. This approach leads to a larger thrust generation and higher utilization of the magnetic field energy. To suppress magnetic leakage and improve the interaction force between the permanent magnets, the outermost ring is wrapped in insulating material. By adjusting the number of unit cells, while ensuring that both the radial and axial dimensions meet the required specifications, the magnetic circuit can be tailored to create structures that range from two-layer nested two-pole crossover to eight-layer nested eight-pole crossover. This flexibility allows the bearing to meet the performance needs of different application scenarios.

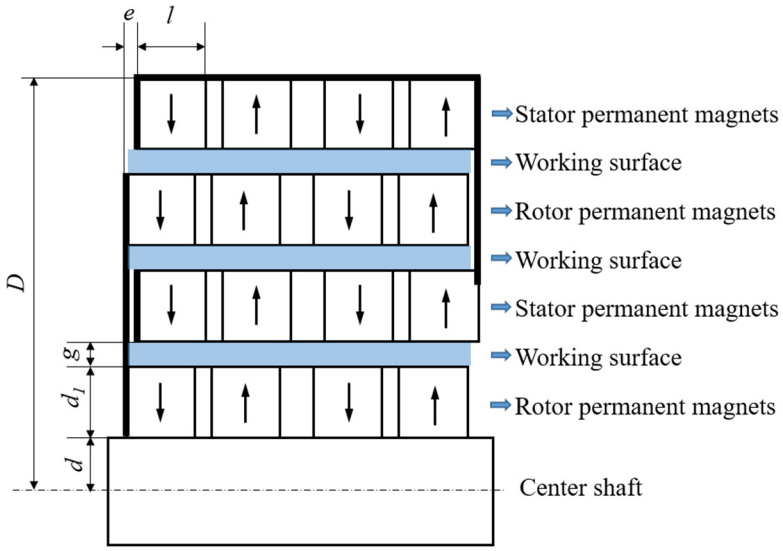


Figure 7. Four-layer nested four-pole crossover bearing magnetic circuits. The arrows in the diagram represent the direction of the magnetic lines of force.

3.2. Theoretical Models

In order to calculate the bearing capacity of a permanent magnet thrust bearing theoretically, the first step is to construct the theoretical model of the bearing. A large body of research has demonstrated that the equivalent magnetic circuit method is an effective and reliable approach for analyzing the magnetic field distribution and magnetic force in permanent magnet bearings [22]. Through the equivalent magnetic circuit model, the mathematical expression of the axial magnetic force in permanent magnet bearings can be established. From this, parameters such as axial stiffness and other mechanical properties of the bearing can be derived.

The core idea behind the equivalent magnetic circuit method is to draw an analogy between the magnetic parameters, such as magnetic flux, magnetic potential, and magnetic resistance, in the permanent magnets and the elements of an electrical circuit—specifically, electric potential, current, and resistance. By simplifying the magnetic circuit in this way, the method allows for efficient calculations with high accuracy [23]. This approach not only streamlines the process of calculating the magnetic forces but also provides a practical and precise means of evaluating the performance of permanent magnet thrust bearings.

Equivalent Magnetic Circuit Model

The N-layer nested N-pole crossover permanent magnet thrust bearing contains $N/2$ layers of the rotor and $N/2$ layers of the stator, and each layer, in turn, contains N rings of permanent magnets with opposite magnetization directions. The two adjacent layers of permanent magnets generate four layers of suction and three layers of repulsion when generating small axial displacements e, ignoring the force between the non-adjacent permanent magnets. In the modeling, in order to improve the computational efficiency, the magnetic leakage of the two end surfaces of the permanent magnet bearings and the outermost layer is ignored, the magnetic leakage of the rotor and stator air gap parts are ignored, and the central axis is also taken as a benign magnetically conductive material, and its magnetic resistance is ignored. The N-layer nested N-pole crossover permanent magnet thrust bearing model constructed by the equivalent magnetic circuit method is shown in Figure 8, which includes the N-layer cross-nested structure of the permanent magnet permeability and the N-1-layer air gap permeability.

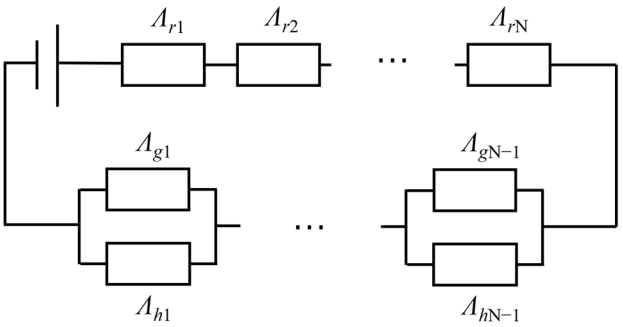


Figure 8. Equivalent magnetic circuit model of N-layer nested N-pole crossover permanent magnet thrust bearing.

3.3. Calculation of Magnetic Permeability

Based on the equivalent magnetic circuit model of the permanent magnet thrust bearing, the total magnetic permeability of the bearing mainly consists of the permanent magnet ring permeability and the air gap permeability, in which the permanent magnet ring permeability can be expressed according to the magnetic permeability equation [24]:

$$\Lambda = 2\mu\pi L / \ln(R_2/R_1) \tag{1}$$

where R_1 and R_2 are the radii of the outer and inner rings of the permanent magnet ring, respectively, L is the axial length of the permanent magnet ring, and μ is the permeability, the value of which can be calculated from the remanent magnetization and coercivity of the permanent magnet [25].

For a permanent magnet bearing with an N-layer nested structure, the permeability of the kth layer of the permanent magnet ring is

$$\Lambda_{rk} = \frac{2\mu\pi L_n}{\ln\left\{\frac{d+kd_1+(k-1)h_g}{d+(k-1)(d_1+h_g)}\right\}} \tag{2}$$

where L_n is the length of the permanent magnet ring in the axial direction, d is the radius of the center axis of the permanent magnet bearing, d_1 is the thickness of the permanent magnet in the radial direction, and h_g is the air gap of the permanent magnet bearing.

For the air gap permeability of the permanent magnet bearing, it is also necessary to consider the change of the air gap area under the action of the bearing for axial displacement. When the axial displacement e is generated, according to the principle of virtual displacement [26], the magnetic line length of the air gap between the two permanent magnet rings of the permanent magnet bearing has h_g change:

$$l = \sqrt{h_g^2 + e^2} \tag{3}$$

The change of the length of the magnetic force line leads to the equivalent cross section S of the magnetic flux expressed as follows:

$$S = \frac{2\pi(R + h_g/2)L_n h_g}{\sqrt{{h_g}^2 + e^2}} \tag{4}$$

According to the magnetic permeability formula and considering the difference of suction and repulsion between the air gaps, the kth layer suction air gap permeability Λ_{gk}

and the kth layer repulsion air gap permeability of the permanent magnet bearing Λ_{hk} can be expressed as follows:

$$\Lambda_{gk} = \frac{2\mu_0\pi\left[d + kd_1 + (1 + k/2)h_g\right]L_n h_g}{h_g^2 + e^2} \tag{5}$$

$$\Lambda_{hk} = \frac{2\mu_0\pi\left[d + kd_1 + (1 + k/2)h_g\right]L_{n-1} h_g}{h_g^2 + e^2} \tag{6}$$

Based on the above analysis, the total permeability of the permanent magnet bearing can be calculated from the superposition of the N-layer nested structure of the permanent magnet permeability and the N-1 layer air gap permeability:

$$\begin{aligned} \frac{1}{\Lambda_a} &= \sum_{k=1}^{N} \frac{1}{\Lambda_{rk}} + \sum_{k=1}^{N-1} \frac{1}{\Lambda_{gk} + \Lambda_{hk}} \\ &= \sum_{k=1}^{N} \frac{\ln\left\{\dfrac{d + kd_1 + (k-1)h_g}{d + (k-1)(d_1 + h_g)}\right\}}{2\mu\pi L_n} \\ &+ \sum_{k=1}^{N-1} \frac{h_g^2 + e^2}{2\mu_0\pi\left[d + kd_1 + \left(\dfrac{2+k}{2}\right)h_g\right](L_n + L_{n-1})h_g} \end{aligned} \tag{7}$$

3.4. Calculation of Bearing Capacity of Permanent Magnet Thrust Bearing

In order to calculate the stiffness characteristics of the permanent magnet bearing, the first step is to determine the bearing capacity index under the action of axial displacement. In the operation of a permanent magnet bearing, an axial load is applied when a small axial displacement, denoted as e, occurs. At this point, the attractive and repulsive forces in the air gap between the permanent magnets hinder the axial movement of the rotor. The force that resists this displacement is referred to as the bearing capacity of the permanent magnet bearing.

For permanent magnet thrust bearings, the permanent magnet material is typically NdFeB (neodymium iron boron), which exhibits high magnetic strength. The air gap load line and demagnetization line for the permanent magnet material are depicted in Figure 9. The working point of the permanent magnet, denoted as P, represents the point on the air gap load line at which the bearing operates under the applied axial displacement. The relationship between these forces governs the bearing's load-carrying capacity and stiffness characteristics. Understanding the interaction between the axial displacement and the magnetic forces in the air gap is crucial for calculating the bearing capacity and stiffness of the permanent magnet thrust bearing. This enables engineers to optimize the design and performance of the bearing in various applications.

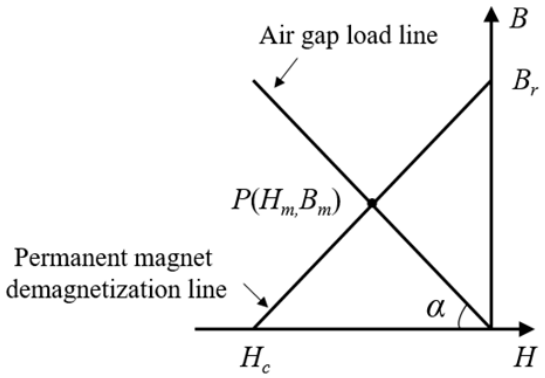


Figure 9. Air gap loading lines and demagnetization lines of permanent magnetic materials.

According to the principle of the magnetic circuit of a permanent magnet [27], the magnetic flux density at the working point of a permanent magnet can be expressed as follows:

$$B_m = \frac{B_r H_c d_1 \Lambda}{B_r S + H_c d_1 \Lambda} \tag{8}$$

where B_r is the remanent magnetic induction of the permanent magnet, H_c is the coercive force of the permanent magnet, d_1 is the thickness of the permanent magnet in the radial direction, and S is the cross-sectional area of the magnetic circuit of the magnetic ring.

According to the flux continuity principle [28], the radial flux of the k-layer gap of the permanent magnet thrust bearing is

$$\Phi_{gk} = \frac{2\pi R_k n l B_r H_c d_1 \Lambda}{2\pi R_k n l B_r + H_c d_1 \Lambda} \tag{9}$$

where R_k is the equivalent radius of the kth layer permanent magnet ring.

The gap magnetic energy of the kth layer permanent magnet ring can be obtained by a flux and permeability calculation:

$$W_g = \Phi_g^2 / 2\Lambda \tag{10}$$

Based on the principle of the virtual work of the permanent magnet bearing in the working process [29], the axial magnetic force generated by the permanent magnet ring can be expressed as follows:

$$F_z = \frac{\partial W_g}{\partial e} = -\frac{\Phi_g^2}{2\Lambda_g^2} \times \frac{\partial \Lambda_g}{\partial e} \tag{11}$$

Based on the above analysis, the axial magnetic force generated by the suction of the kth ring gap is

$$F_{gk} = \frac{\left(\frac{2\pi R n l B_r H_c d_1 \Lambda_a}{2\pi R n l B_r + H_c d_1 \Lambda_a}\right)^2 e^2}{2\mu_0 \pi \left[d + k d_1 + (1 + k/2) h_g\right] L_n h_g} \tag{12}$$

The axial magnetic force generated by the repulsive of the kth ring gap is

$$F_{hk} = \frac{\left(\frac{2\pi R n l B_r H_c d_1 \Lambda_a}{2\pi R n l B_r + H_c d_1 \Lambda_a}\right)^2 e^2}{2\mu_0 \pi \left[d + k d_1 + (1 + k/2) h_g\right] L_{n-1} h_g} \tag{13}$$

The combined force in the axial direction of the permanent magnet thrust bearing is

$$\begin{aligned} F_e &= \sum_{k=1}^{N-1} F_{gk} + \sum_{k=1}^{N-1} F_{hk} \\ &= \sum_{k=1}^{N-1} \left\{ \frac{\left(\frac{2\pi R n l B_r H_c d_1 \Lambda_a}{2\pi R n l B_r + H_c d_1 \Lambda_a}\right)^2 e^2}{2\mu_0 \pi \left[d + k d_1 + \left(\frac{2+k}{2}\right) h_g\right] L_n h_g} \right\} \\ &+ \sum_{k=1}^{N-1} \left\{ \frac{\left(\frac{2\pi R n l B_r H_c d_1 \Lambda_a}{2\pi R n l B_r + H_c d_1 \Lambda_a}\right)^2 e^2}{2\mu_0 \pi \left[d + k d_1 + \left(\frac{2+k}{2}\right) h_g\right] L_{n-1} h_g} \right\} \end{aligned} \tag{14}$$

3.5. Calculation of the Stiffness of Permanent Magnet Thrust Bearing

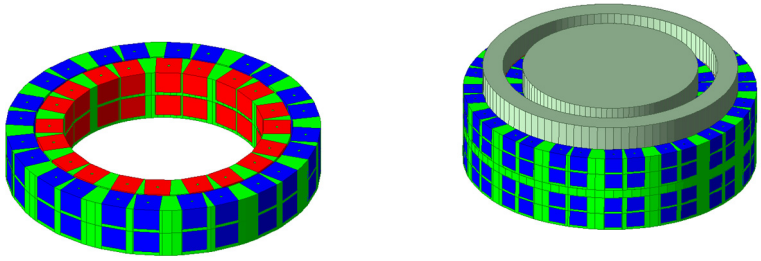
During the operation of permanent magnet thrust bearing, the rotor is slightly deflected under the axial load e. The axial magnetic force of the permanent magnet bearing

prevents the rotor from generating displacement, defining the stiffness of the permanent magnet thrust bearing as the ratio of the magnetic force to the rotor deflection e. Therefore, the stiffness of the bearing can be expressed as follows:

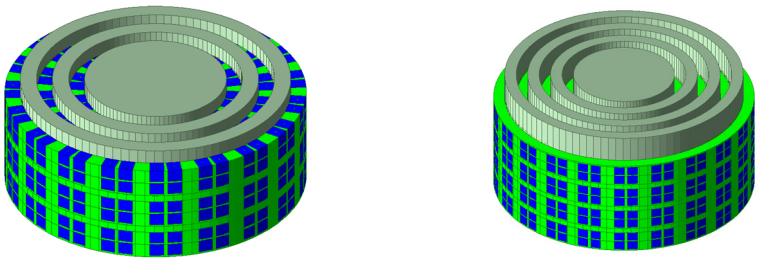
$$\begin{aligned} K &= \frac{\partial F_e}{\partial e} \\ &= \sum_{k=1}^{N-1} \left\{ \frac{\left(\frac{2\pi RnlB_r H_c d_1 \Lambda_a}{2\pi RnlB_r + H_c d_1 \Lambda_a} \right)^2 e}{\mu_0 \pi \left[d + kd_1 + \left(\frac{2+k}{2} \right) h_g \right] L_n h_g} \right\} \\ &+ \sum_{k=1}^{N-1} \left\{ \frac{\left(\frac{2\pi RnlB_r H_c d_1 \Lambda_a}{2\pi RnlB_r + H_c d_1 \Lambda_a} \right)^2 e}{\mu_0 \pi \left[d + kd_1 + \left(\frac{2+k}{2} \right) h_g \right] L_{n-1} h_g} \right\} \end{aligned} \tag{15}$$

4. Simulation Analysis

Finite element simulation is an important means of performance verification at the product design stage. In order to verify the load-carrying characteristics of the proposed modular multi-unit cell permanent magnet thrust bearing, four types of structures were developed based on the concepts of modularity and generalization. These included a two-layer nested two-pole crossover, a four-layer nested four-pole crossover, a six-layer nested six-pole crossover, and an eight-layer nested eight-pole crossover bearing. All models were constructed using commercial finite element software, and their bearing characteristics were analyzed. The different models utilize a generalized and modular unit cell structure, varying only in the number and arrangement of unit cells. This approach aimed to demonstrate the load-bearing characteristics of different layer nested and pole crossover configurations. The simulation models of the different structures are illustrated in Figure 10. The red block indicates the rotor and the blue color indicates the stator.



(**a**) Two-layer nested two-pole crossover (**b**) Four-layer nested four-pole crossover



(**c**) Six-layer nested six-pole crossover (**d**) Eight-layer nested eight-pole crossover

Figure 10. Simulation models of bearings with different structures.

Since the magnetic permeability of adiabatic materials and air in Ansoft/Maxwell 2023R1 software is almost identical, the basic structure of the bearing was simplified during

the modeling process. The rotor and stator seats were excluded, and only the rotor and stator chokes, block mounting baskets, and permanent magnet blocks were retained. The four structural bearing models were then created by adjusting the number of permanent magnet blocks and their arrangement based on the number of layers in the rotor and stator. For the simulation, the motion domain settings of the permanent magnet thrust bearing were as follows: The rotor was assigned a motion domain, with the bearing speed set to 180 rpm. The axial displacement of the rotor was set to range from 2 mm to 30 mm, with a step size of 1 mm.

The basic parameters of the bearings are outlined in Table 1. Given these parameters, the neutral axis diameter of bearings with different structures was consistent, and the performance characteristics of the permanent magnets were identical. The air gap between the permanent magnet rings was set at 2 mm. Additionally, the quantity of permanent magnets and unit cells varied among different structural configurations. The maximum diameter of the bearing was related to the number of nested layers, while the axial length was determined by the number of cross layers in the bearing. These parameters for different bearing structures are also summarized in Table 1. This modeling and simulation approach enabled the evaluation of various structural configurations and their corresponding bearing characteristics, such as load capacity, stiffness, and displacement response.

Table 1. Basic parameters of bearings with different structures.

Bearing Parameters	Two-Layer Nested Two-Pole Crossover	Four-Layer Nested Four-Pole Crossover	Six-Layer Nested Six-Pole Crossover	Eight-Layer Nested Eight-Pole Crossover
Center shaft diameter (mm)	110	110	110	110
Maximum diameter (mm)	234	362	490	618
Magnet thickness (mm)	30	30	30	30
Magnet length (mm)	28	28	28	28
Axial length (mm)	113	185	257	329
Permanent magnet grades	N48	N48	N48	N48
Residual magnetism	1.4 T	1.4 T	1.4 T	1.4 T
Number of permanent magnets	88	416	1044	2096
Number of unit cells	22	104	261	524
Ring gap (mm)	2	2	2	2
Axial displacement (mm)	2–30	2–30	2–30	2–30

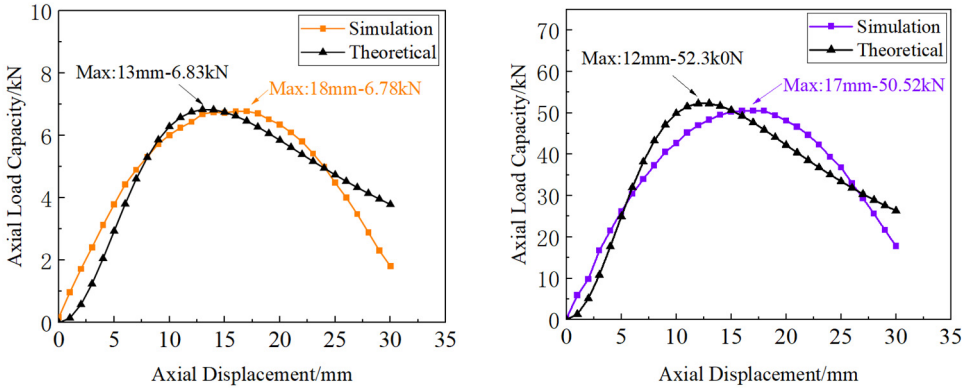
Based on Ansoft/Maxwell software, simulation verification of bearings with different structures was carried out to analyze the bearing performance in the interval of axial displacement of 2–30 mm and the maximum bearing capacity of each layer was superimposed by Equation (16), to find out the maximum axial bearing capacity of the bearing as a whole.

$$F = \sum_{1}^{k} F_k + \sum_{1}^{l} F_l \tag{16}$$

where F is the maximum total bearing capacity of the bearing, k and l denote the number of layers of the rotor and stator, respectively, and F_k and F_l are the bearing capacity of the kth layer of the rotor and the lth layer of the stator, respectively.

The bearing capacity of permanent magnet thrust bearings with different structures is shown in the Figure 11 by comparing the finite element simulation results with the theoretical model. Overall, the axial bearing capacity of the bearing first increases and then

decreases with the increase of axial displacement. This is because as the axial displacement of the bearing increases, the attraction and repulsion between the permanent magnets increase, limiting the further increase of the axial displacement. However, as the axial displacement continues to increase, the outermost layer of permanent magnets will gradually leave the working surface, resulting in a reduction in the working area and a decrease in the number of layers of permanent magnets that interact. This ultimately leads to a decrease in its axial bearing capacity. In addition, the images indicate that the maximum bearing capacity of the theoretical model is greater than that of the simulation model. This discrepancy arises from the construction of the equivalent magnetic circuit model, where the leakage flux from the outermost layer and the air gap is neglected. Additionally, the shaft material is treated as an ideal magnetic conductor, and its magnetic resistance is not considered. Consequently, the results of the theoretical analysis are higher than those obtained from the simulations. Moreover, in the theoretical model, the axial length of the permanent magnet bearing is calculated based on the combined length of four layers of permanent magnet rings, without accounting for the length of the unit cell. This leads to a difference in the axial displacement associated with the maximum bearing capacity of the two models. For the single structure bearing, the errors between the theoretical and simulation models are 0.7%, 3.5%, 1.2%, and 2%, respectively.



(**a**) Two-layer nested two-pole crossover (**b**) Four-layer nested four-pole crossover

(**c**) Six-layer nested six-pole crossover (**d**) Eight-layer nested eight-pole crossover

Figure 11. Carrying capacity of permanent magnet thrust bearing with different structures.

According to the simulation results, the unit cell bearing capacity and unit magnet block bearing capacity for different structures of the permanent magnet thrust bearing are shown in Table 2. As the number of nested and cross layers in the bearing increases, both the unit cell and the unit magnet block bearing capacity also increase. This trend can be attributed to the higher ratio of the number of magnet layers to the working surface in the multilayer structure, which leads to a more efficient utilization of the magnetic field.

Table 2. Indicators of the load-carrying capacity of bearings of different structures.

Carrying Capacity Indicators	Two-Layer Nested Two-Pole Crossover	Four-Layer Nested Four-Pole Crossover	Six-Layer Nested Six-Pole Crossover	Eight-Layer Nested Eight-Pole Crossover
Unit cell (kN)	0.308	0.486	0.524	0.551
Unit magnet block (kN)	0.077	0.121	0.131	0.138

The increased magnet utilization in the multilayer cross-nested structure enhances the overall bearing capacity, as reflected in the higher unit cell and unit magnet block bearing capacities. These results validate the advantages of the multilayer cross-nested structure in improving the bearing's load-carrying performance. By effectively using the available magnetic flux and optimizing the distribution of magnetic forces, the proposed structure significantly enhances the bearing's overall efficiency and capacity.

5. Experimental Validation

Experimental verification technology is one of the key technologies for permanent magnet thrust bearings. To verify the accuracy of the theoretical derivations and finite element simulations, a test bed for permanent magnet thrust bearings was constructed based on the application scenario of permanent magnet thrust bearings in ship spindle propulsion. The experimental platform, shown in Figure 12, mainly consists of the following components: a four-layer nested four-pole crossover permanent magnet thrust bearing, a motorized pusher that controls the displacement of the bearing rotor, a rotor-driven rotating motor, and sensors for force, displacement, and torque.

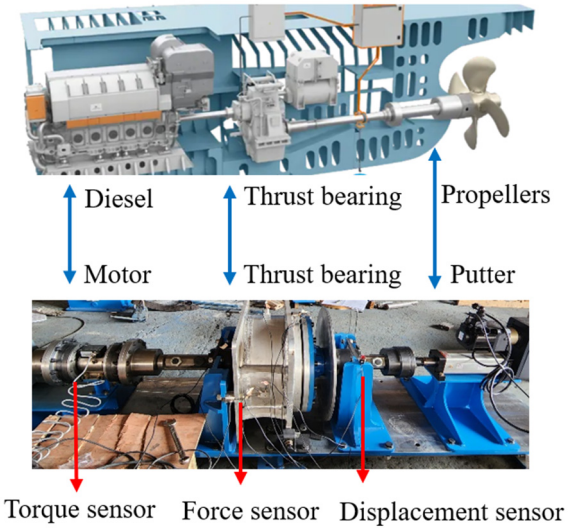


Figure 12. Permanent magnet thrust bearing test bed and bearing prototype.

In the experiment design, a motor rotates the rotor at 180 r/min to simulate the rotational speed of a ship's diesel engine propulsion system. Meanwhile, an electric actuator moves the bearing rotor to a specified displacement to mimic the reaction force of the ship's propeller propulsion. The displacement range is from 2 mm to 25 mm, with a step size of 1 mm. Sensors for force, displacement, and torque continuously monitor the status of the experimental platform in real-time. This experimental setup is crucial for verifying the correctness of theoretical and simulation results and provides valuable data for evaluating the performance of permanent magnet thrust bearings in practical applications.

Experimental Verification of Load-Carrying Performance of Permanent Magnet Thrust Bearing

According to the experiments conducted on the constructed four-layer nested four-pole crossover permanent magnet thrust bearing prototype and bearing test bed, different displacements were achieved by controlling the electric actuator, and the axial bearing capacity was recorded. By differentiating the bearing capacity with respect to displacement, the experimental rigidity of the permanent magnet thrust bearing can be derived. The theoretical, simulation, and experimental values of the bearing capacity of the permanent magnet thrust bearing are shown in Figure 13. The bearing capacity of the permanent magnet thrust bearing first increases and then decreases, with an effective working range of 2–15 mm. In the theoretical calculation, the maximum bearing capacity of the permanent magnet thrust bearing is 52.30 kN, which occurs at an axial displacement of 12 mm. In the finite element simulation, the maximum bearing capacity is 50.52 kN, corresponding to an axial displacement of 17 mm. In the experimental results, the maximum bearing capacity of the permanent magnet thrust bearing prototype is 48.45 kN. The error compared to the theoretical value is 7.3%, and the error compared to the simulation solution is 4%. The sources of error can be summarized in three areas. The first is an error in the equivalent magnetic circuit model at the time of construction. In the construction of the equivalent magnetic circuit model, the magnetic leakage of the outermost layer and the air gap part is neglected, and at the same time, the material of the central axis is approximated as a benign magnetically conductive material, and its magnetoresistance is neglected, so the results of the theoretical analysis may be larger than the experimental results. At the same time, in the theoretical model, the axial length of the PM bearing is calculated according to the length of the four-layer PM ring, and the length of the cytoskeleton is neglected, so there may be a certain amount of difference in the axial displacements corresponding to the maximal bearing capacity of the two models. The second area is a manufacturing or assembly error in the test prototype. The standard prototype magnet blocks are uniformly arranged in the axial and radial directions; however, due to the limitations of the manufacturing means and assembly process, there may be an unevenness in the axial and radial gaps between the magnet blocks, which directly affects the real reluctance of the bearings and other parameters. The third area is an error in the experimental process. Due to the experimental device being relatively rough, the installation and debugging of the sensors may not be precise enough, and there may be a difference in the experimental process.

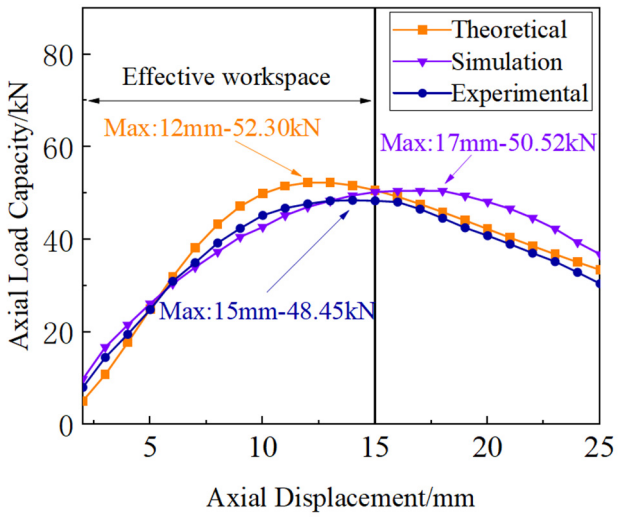


Figure 13. Comparison of load-carrying capacity of permanent magnet thrust bearing.

The theoretical solution, simulation solution, and experimental values of the stiffness of the permanent magnet thrust bearing are shown in Figure 14. As the axial displacement

increases, the stiffness of the bearing initially increases and then decreases. At 15 mm, the stiffness becomes negative. This is because the axial length of the permanent magnets is 30 mm, and when the rotor's axial displacement reaches 15 mm, the axial bearing capacity reaches its maximum. However, with further increases in axial displacement, the outermost permanent magnets gradually disengage from contact, causing the magnetic circuit's cross-sectional area to narrow. As a result, the bearing capacity diminishes with the increase in axial displacement, and the maximum displacement cannot exceed 15 mm during the operation of the permanent magnet bearing. In terms of the stiffness values, the theoretical, simulation, and experimental results show that the maximum error of the experimental stiffness in the positive stiffness stage is 17.2% relative to the theoretical value and 23.9% relative to the simulation value. These discrepancies are mainly due to deviations in the actual parameters of the permanent magnets compared to the theoretical parameters, as well as manufacturing and assembly errors during the construction of the prototype.

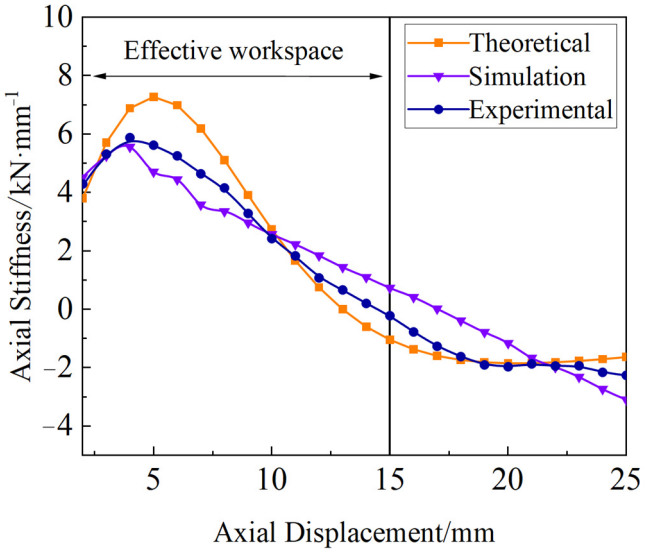


Figure 14. Stiffness comparison of permanent magnet thrust bearing.

6. Conclusions

In order to improve the load-carrying capacity and versatility of the permanent magnet thrust bearing, this paper has proposed a new modular multi-unit cell permanent magnet thrust bearing based on the design concept of bionics and a modular design scheme. By generalizing the unit cell structure, it can be constructed according to varying requirements, with different layers of nested and cross permanent magnet thrust bearings. The proposed bearing has been verified through theoretical calculations, finite element simulations, and experimental testing.

(1) Based on the design concept of bionics and referring to the structure of honeycombs, this paper adopted a modular and unit cell (composed of four permanent magnets and made universal) combination approach to construct different nested and cross structural configurations of permanent magnet thrust bearings, thereby enhancing the adaptability of permanent magnet thrust bearings in different scenarios.

(2) The theoretical model of the novel modular multi-unit cell permanent magnet thrust bearing was developed using the equivalent magnetic circuit method. By applying the principles of virtual displacement and virtual work, computational expressions for bearing capacity and stiffness were established. This theoretical model extends the traditional single-layer cross-nested structure to accommodate multi-layer cross-nested configurations, improving the model's applicability.

(3) The bearing performance of the proposed permanent magnet thrust bearing was verified through finite element simulations and experimental testing. Based on the practical application scenario of ship spindle propulsion, a permanent magnet thrust bearing experimental platform was built, and a modular permanent magnet thrust bearing with a four-layer cross-nested structure was constructed for validation. The experimental results show that the maximum bearing capacity of the prototype is 48.45 kN, with a 7.3% error relative to the theoretical value and a 4% error relative to the simulation solution, demonstrating good accuracy.

Benefiting from the advantages of permanent magnet thrust bearings, such as quiet operation, vibration damping, and high rotational speed, this paper expands the traditional low-load permanent magnet thrust bearing to higher load ranges. The proposed modular multi-unit cell permanent magnet thrust bearing shows promising potential for applications in ship spindle propulsion. However, the existing range of applications for permanent magnet thrust bearings is still limited. Furthermore, due to the large quantity of permanent magnet materials used, the cost remains high compared to traditional bearings. In future research, efforts should focus on reducing the use of permanent magnet materials while maintaining load-carrying performance, in order to improve the competitiveness of permanent magnet thrust bearings in the market. The permanent magnet thrust bearing designed in this paper is a passive system. In the future, researchers in this field can explore the combination of permanent magnets and active control systems for the design of permanent magnet thrust bearings, so that the high efficiency of permanent magnets and the high precision of active control systems can be utilized at the same time, for example, the use of a passive permanent magnet structure in the substrate structure, and the use of active control systems in axial and radial precision control, so that a larger load-bearing capacity can be achieved based on the artificial active control system stiffness and other properties to meet the needs of more scenarios/conditions. This would allow the use of an active control system for precise axial and radial control, thus realizing a higher load-carrying capacity and artificial stiffness of the active control system to meet the needs of more scenarios/properties.

Author Contributions: Conceptualization, X.Y. and W.Y.; Methodology, X.Y. and W.Y.; Software, Q.W., Z.Y. and X.S.; Validation, X.Y., Q.W., Z.Y. and S.Z.; Formal analysis, Q.W. and X.S.; Investigation, X.S.; Resources, Z.Y. and S.Z.; Writing – original draft, S.Z.; Supervision, W.Y. and J.Z.; Funding acquisition, J.Z. All authors have read and agreed to the published version of the manuscript.

Funding: This research received no external funding.

Institutional Review Board Statement: Not applicable.

Informed Consent Statement: Not applicable.

Data Availability Statement: The original contributions presented in this study are included in the article. Further inquiries can be directed to the corresponding author.

Conflicts of Interest: The authors declare no conflict of interest.

References

1. Praharaj, R.K.; Datta, N. Application of fractional calculus in modelling viscoelastic foundation of ship structures for passive vibration control. In Proceedings of the ASME 39th International Conference on Ocean, Offshore and Arctic Engineering (OMAE), Online, 3–7 August 2020.
2. Lu, Z.; Liang, Q.; Zhou, Y.; Luo, W.; Li, J.; Jiang, K. Novel Thick Layer Damping Rubber Bearing (TLDRB) with reduced vertical stiffness: Laboratory tests and mechanical models. *J. Build. Eng.* **2024**, *94*, 109839.
3. Shao, C.; Wen, H.; Peng, Z.; Lin, K.; Zeng, L.; Chen, W. Influences of Special Hydraulic Device on the Longitudinal Vibration Characteristics of Ship Shafting. *Ship Eng.* **2021**, *43*, 10–15.

4. Qin, Y.; Huang, Z.; Wu, Z.; Yang, K. Vibration Reduction Application of Piezoelectric-damping Composite on the Hull Loading Capacity Bearing. *J. Wuhan Univ. Technol.* **2012**, *34*, 1–4.
5. Tang, J.; Fang, J.; Tong, W. Superconducting Magnetic Bearings and Active Magnetic Bearings in Attitude Control and Energy Storage Flywheel for Spacecraft. *IEEE Trans. Appl. Supercond.* **2012**, *22*, 5702109.
6. Murakami, K.; Komori, M.; Mitsuda, H.; Inoue, A. Design of an energy storage flywheel system using permanent magnet bearing (PMB) and superconducting magnetic bearing (SMB). *Cryogenics* **2007**, *47*, 272–277. [CrossRef]
7. Yu, Y.; Zhang, W.; Sun, Y.; Xu, P. Basic Characteristics and Design of a Novel Hybrid Magnetic Bearing for Wind Turbines. *Energies* **2016**, *9*, 905. [CrossRef]
8. Dagnaes-Hansen, N.A.; Santos, I.F. Permanent magnet thrust bearings for flywheel energy storage systems: Analytical, numerical, and experimental comparisons. *Proc. Inst. Mech. Eng. Part C J. Mech. Eng. Sci.* **2019**, *233*, 5280–5293. [CrossRef]
9. Hirani, H.; Samanta, P. Hybrid (hydrodynamic plus permanent magnetic) journal bearings. *Proc. Inst. Mech. Eng. Part J J. Eng. Tribol.* **2007**, *221*, 881–891.
10. Guo, K.; Rao, X. Research and Realization on Automation Modeling of the Centrifuge Permanent Magnetic Bearing Simulation System. *J. Donghua Univ. Nat. Sci. Ed.* **2007**, *33*, 298–301.
11. Zhou, D.; Zhang, G. Study on mechanical properties of radial permanent magnet bearing. In Proceedings of the IEEE International Conference on Cybernetics and Intelligent Systems (CIS)/IEEE Conference on Robotics, Automation and Mechatronics (RAM), Ningbo, China, 19–21 November 2017.
12. Zhao, W.J.; Mei, L. Research on Modular Permanent Magnet Bias Magnetic Bearing. In Proceedings of the 24th International Conference on Electrical Machines and Systems (ICEMS), Gyeongju, Republic of Korea, 31 October–3 November 2021.
13. Xiao, L.; He, X.; Cheng, W.; Fan, H.; Li, M. Optimization and dynamic characteristics of a new type of permanent magnet bias bearing. *Proc. Inst. Mech. Eng. Part C J. Mech. Eng. Sci.* **2020**, *234*, 4366–4376.
14. Van Beneden, M.; Kluyskens, V.; Dehez, B. Optimal Sizing and Comparison of Permanent Magnet Thrust Bearings. *IEEE Trans. Magn.* **2016**, *53*, 8300110. [CrossRef]
15. Štumberger, B.; Štumberger, G.; Hadžiselimović, M.; Hamler, A.; Goričan, V.; Jesenik, M.; Trlep, M. Comparison of torque capability of three-phase permanent magnet synchronous motors with different permanent magnet arrangement. *J. Magn. Magn. Mater.* **2007**, *316*, E261–E264. [CrossRef]
16. Stumberger, B.; Pulko, R.; Gorican, V.; Hadziselimovic, M. Influence of permanent magnet material on characteristics of permanent magnet assisted reluctance motor. *Prz. Elektrotechniczny* **2010**, *86*, 142–144.
17. Yue, M.; Zhang, X.; Liu, J.P. Fabrication of bulk nanostructured permanent magnets with high energy density: Challenges and approaches. *Nanoscale* **2017**, *9*, 3674–3697. [CrossRef]
18. Boldea, I.; Tutelea, L.N.; Parsa, L.; Dorrell, D. Automotive Electric Propulsion Systems With Reduced or No Permanent Magnets: An Overview. *IEEE Trans. Ind. Electron.* **2014**, *61*, 5696–5711. [CrossRef]
19. Sun, X.; Xu, N.; Yao, M. Sequential Subspace Optimization Design of a Dual Three-Phase Permanent Magnet Synchronous Hub Motor Based on NSGA III. *IEEE Trans. Transp. Electrif.* **2022**, *9*, 622–630. [CrossRef]
20. Rodriguez, E.; Sotelo, G.G.; De Oliveira, J.G.; De Santiago, J.; Rossander, M.; Stephan, R. Designing, simulations and experiments of a passive permanent magnet bearing. *Int. J. Appl. Electromagn. Mech.* **2016**, *51*, 131–149.
21. Wajnert, D.; Tomczuk, B. Two Models for Time-Domain Simulation of Hybrid Magnetic Bearing's Characteristics. *Sensors* **2022**, *22*, 1567. [CrossRef]
22. Liu, X.; Dong, J.; Du, Y.; Shi, K.; Mo, L. Design and Static Performance Analysis of a Novel Axial Hybrid Magnetic Bearing. *IEEE Trans. Magn.* **2014**, *50*, 8300404. [CrossRef]
23. Han, B.; Xu, Q. Design, Modeling, and Performance Testing of a Weak Coupling Combined Radial-Axial Magnetic Bearing. *J. Eng. Gas Turbines Power-Trans. ASME* **2015**, *137*, 102503.
24. Le, Y.; Fang, J.; Han, B.; Zhang, Y. Dynamic circuit model of a radial magnetic bearing with permanent magnet bias and laminated cores. *Int. J. Appl. Electromagn. Mech.* **2014**, *46*, 43–60. [CrossRef]
25. Kulan, M.C.; Baker, N.J. Fast Analytical Force Estimation in Active Magnetic Bearings using a Magnetic Equivalent Circuit Model. In Proceedings of the IEEE International Electric Machines and Drives Conference (IEMDC), San Francisco, CA, USA, 15–18 May 2023.
26. Wajnert, D.; Sykulski, J.K.; Tomczuk, B. An Enhanced Dynamic Simulation Model of a Hybrid Magnetic Bearing Taking Account of the Sensor Noise. *Sensors* **2020**, *20*, 1116. [CrossRef] [PubMed]
27. Dong, L.; Qian, J.; Wang, C.; Wang, X.; Wu, M. Improving Magnetic Circuit Calculation for Magnetic Thrust Bearing. *J. Shanghai Univ. (Nat. Sci.)* **2005**, *11*, 375–380.

28. Han, B.; Zheng, S.; Le, Y.; Xu, S. Modeling and Analysis of Coupling Performance Between Passive Magnetic Bearing and Hybrid Magnetic Radial Bearing for Magnetically Suspended Flywheel. *IEEE Trans. Magn.* **2013**, *49*, 5356–5370. [CrossRef]
29. Zhang, T.; Ye, X.; Mo, L.; Liu, X. Modeling and Performance Analysis on the Slice Hybrid Magnetic Bearing With Two Radial Air-Gaps. *IEEE Trans. Appl. Supercond.* **2019**, *29*, 3601105. [CrossRef]

Disclaimer/Publisher's Note: The statements, opinions and data contained in all publications are solely those of the individual author(s) and contributor(s) and not of MDPI and/or the editor(s). MDPI and/or the editor(s) disclaim responsibility for any injury to people or property resulting from any ideas, methods, instructions or products referred to in the content.